Korean J. Chem. Eng., 34(5), 1377-1384 (2017)
DOI: 10.1007/s11814-016-0337-6

pISSN: 0256-1115
eISSN: 1975-7220

Removal of chlorinated phenol from aqueous solution utilizing activated carbon derived from papaya (*Carica Papaya)* seeds

Duduku Krishnaiah*,†, Collin G. Joseph, S. M. Anisuzzaman*, W. M. A. W. Daud***, M. Sundang*, and Y. C. Leow****

*Chemical Engineering Programme, Faculty of Engineering, Universiti Malaysia Sabah, Jln UMS, 88400 Kota Kinabalu, Sabah, Malaysia
**Water Research Unit, Faculty of Science & Natural Resources, Universiti Malaysia Sabah, Jln UMS, 88400 Kota Kinabalu, Sabah, Malaysia
***Department of Chemical Engineering, Faculty of Engineering, University of Malaya, 50603 Kuala Lumpur, Malaysia
(*Received 8 June 2016 • accepted 29 November 2016*)

Abstract−Activated carbons (ACs) were prepared from papaya seeds with different dry weight impregnation ratios of zinc chloride ($ZnCl_2$) to papaya seeds by using a two-stage self-generated atmosphere method. The papaya seeds were first semi-carbonized in a muffle furnace at 300 °C for 1 h and then impregnated with $ZnCl_2$ before activation at 500 °C for 2 h. Several physical and chemical characteristics such as moisture, ash, pH, functional groups, morphological structure and porosity of prepared ACs were studied and presented here. AC2, with the impregnation ration of 1 : 2 (papaya seeds: $ZnCl_2$), yielded a product that had the highest adsorption capacity, 91.75%, achieved after 180 min contact time. The maximum Brunauer, Emmett and Teller (BET) surface area of AC2 was 546 m^2/g. Adsorption studies indicated that AC2 complied well with the Langmuir isotherm (q_m=39.683 mg g^{-1}) and the pseudo-second-order (q_e=29.36 mg g^{-1}). This indicated that chemisorption was the primary adsorption method for AC2. The intraparticle diffusion model proved that the mechanism of adsorption was separated into two stages: the instantaneous stage and the gradual adsorption stage. Overall, this work demonstrated the suitability of using papaya seeds as a precursor to manufacture activated carbon.

Keywords: Activated Carbon, Papaya Seeds, Two Stage Activation, 2,4-Dichlorophenol

INTRODUCTION

Chlorophenols have been classified as organ targetive pollutants due to their toxic affect to the liver, in addition to having carcinogenic and mutagenic effect on human health by the US Environmental Protection Agency (EPA) [1]. The presence of 2,4-dichlorophenol (2,4-DCP) in the environment may occur due to photodecomposition of herbicides or microbial degradation, from chlorination of drinking water and industrial wastewater and municipal wastewater by water disinfection plants, or from agricultural runoff, paper and pulp manufacturing processes or industrial waste discharges [2]. Chlorophenols can penetrate human skin by in vitro and are easily absorbed after oral administration, causing liver and immune systems damage [3].

Biological treatment, photochemical treatment, and air stripping as well as anaerobic granular sludge, catalytic wet oxidation photochemical treatment, fuel oil fly ash, treat incineration, and adsorption technology using activating clay or activated carbon (AC) are the commonly applied approaches in water treatment [4-12]. Fast adsorption kinetics and the simplicity of producing AC are also the reasons for the AC to be the more commonly used in waste water treatment [13]. However, most of the methods have low efficiency in removing the chlorophenols from the water due to the structural stability of the chlorophenols.

Adsorption process by AC is the most efficient way in water treatment technology. The highly microporous structure, large volume and surface area, favorable pore size distribution, thermal stability, capability for rapid adsorption and low acid/base reactivity are the reasons of AC for being an excellent adsorbent [5-9,14]. AC is porous carbon material that can be produced from non-renewable raw materials such as natural coal and renewable raw materials such as acorn shell, bagasse and rice husk, corn cob, barley husk, nutshells, wood sawdust, jackfruit peel, and orange peel. Hence, the production cost of the AC is affected by the conventional heating method and the type of precursor, which limits its use for large scale industrial application. To make AC cost effective, alternative production methods and precursors are needed. AC that can be produced from agricultural wastes is the most suitable precursor to produce low cost AC due to renewable characteristics, high volatile matters and lignocellulosic contents as well as waste utilization [15]. Different types of agriculture by-products have been used as the precursors to prepare AC, such as grape seeds, oil palm shells, sunflower seed oil, pine cone, coffee residue, pomegranate seeds, coconut husk, cocoa shells, cherry stones, and others [1,2,4-8,16-36].

We mainly focused on the preparation of AC from papaya seed, which is an agriculture waste in Malaysia. Papaya is a popular local

†To whom correspondence should be addressed.
E-mail: krishna@ums.edu.my

fruit that is cultivated largely in orchards by individual owners throughout the country. The seeds and skin of this fruit are usually thrown away while the flesh is consumed directly or canned. As a result, the waste materials (seeds and skin) cause disposal and sanitary problems, as the rotting waste attracts flies and animals. For this study, papaya seeds (on a dry weight basis) were impregnated with $ZnCl_2$ at various concentrations ratios. The ash content, moisture content and the yield of the AC were measured and presented to prove the suitability of papaya seeds for AC production. The adsorption capacity, adsorption isotherm and adsorption kinetics of 2,4-DCP by the prepared AC were also studied and analyzed. While the surface functional groups, morphological structure and porosity of prepared ACs were characterized by using Fourier transform infrared spectroscopy (FTIR), scanning electron microscopy (SEM), Brunauer-Emmet-Teller (BET) and Barrett-Joyner-Halenda (BJH) methods, respectively.

MATERIALS AND METHODS

1. Sample Preparation

Papaya seeds from *carica papaya* species were used as a raw material to produce the AC. The papaya seeds as the precursor material were washed with distilled water several times to remove the dirt and slime covering the seeds. The seeds were then dried in an oven for 24 h at 110 °C before being stored for the next step in the process of preparing the ACs.

2. Two-stage Activation Process

There were two main processes in preparation of the AC: the semi-carbonization and chemical activation in the self-generated atmosphere [37]. In the semi-carbonization process, the papaya seeds were heated to 300 °C for about 1 h under self-generated atmosphere and cooled to room temperature in the muffle furnace. The resulting material was labelled as semi-carbonized carbon (SCC). The SCC was then subjected to chemical activation [23]. The SCC was agitated with aqueous solution of 200 mL of zinc chloride ($ZnCl_2$) according to the (wt : wt) of $ZnCl_2$: SCC from 1 : 1 to 5 : 1 (samples AC1-AC5) [24]. The chemical activating agent and precarbonized carbon were homogeneously mixed at 85 °C until the solution was completely dried. The resulting samples were then placed back into the muffle furnace for activation under self-generated atmosphere at the optimum temperature of 500 °C for 2 h before cooling [38].

3. Washing Process

The activated sample was washed with a 0.01 M of HCl solution, then with hot water, at 85 °C for 30 min [38,39]. The pH of each of the samples was recorded. The washed samples were dried for 24 h at 110 °C to obtain the final product.

4. Characterization of AC

Moisture content was determined according to ASTM D2867-04 standard, whereas ash content was determined using ASTM D2866-94 standard. The pH was determined according to ASTM D3838-80 standard. Details for determination percentage of yield, moisture content, ash content and pH were described in our previous work [8,9]. Surface chemistry of the prepared AC was analyzed using FTIR analysis (Thermo Nicolet NEXUS 670) to determine the surface functional groups, where the spectra were recorded in the range of 4,000-650 cm^{-1}. SEM studies (JEOL JSM-5610LV, Japan) at 10 kV with different magnification was used to conduct the morphological study. The specific surface area and the pore-size distribution were determined using the BET and BJH methods. The BET surface area and pore size distribution were determined from nitrogen gas adsorption isotherm at 77.3 K using Quanta chrome autosorb automated gas sorption instrument [7].

5. Adsorption Study

0.5 g of AC samples and 400 mL of 40 mg/L 2,4-DCP were stirred for 3 h to achieve the equilibrium. The samples were extracted and filtered using a Sterlitech 45 μm syringe filter and the solution was analyzed using the UV-Vis spectrophotometer [38]. The AC with highest adsorption capacity was identified and experimented further in batch adsorption experiments. There were three different batch adsorption tests: varying the adsorbent dosage (0.1, 0.3 and 0.5 g), pH (3, 7 and 9) and initial adsorbate concentration (10, 20, 30 and 40 mg L^{-1}). All experiments were done in triplicate with their average values being taken and plotted into graphs.

6. Adsorption Isotherm Study

Langmuir, Freundlich and Temkin isotherms were applied to fit the experimental equilibrium isotherm data to determine the maximum chlorophenol adsorption capacity of prepared carbon [15]. The mathematical expressions of these equations can be written as follows:

$$\text{Langmuir isotherm, } q_e = \frac{q_m K_L C_e}{l + K_L C_e} \tag{1}$$

$$\text{Freundlich isotherm, } q_e = K_F C_e^{1/n} \tag{2}$$

$$\text{Temkin isotherm, } q_e = \frac{RT}{b_T} \ln A_T + \left(\frac{RT}{b}\right) \ln C_e \tag{3}$$

where C_e is the amount of adsorbate in the solution at equilibrium, q_e is the amount of adsorbate adsorbed; q_m is the amount of adsorbate adsorbed to form monolayer coverage, and K_L, n and K_F are the equation constants. A_T is the Temkin isotherm equilibrium binding constant (L/g), b_T is the Temkin isotherm constant, R is universal gas constant, T is temperature (K), b is the constant related to heat of sorption (J/mol). Graphs for C_e/Q_e against C_e; log q_e against log C_e and q_e against lnC_e for Langmuir isotherm; Freundlich isotherm and for Temkin isotherm were plotted, respectively.

7. Adsorption Kinetics Study

Pseudo-first-order, second-order were calculated and plotted to understand the adsorption kinetics in this study. The first-order expression of Lagergren based on solid capacity is defined as:

$$\log(q_e - q_t) = \log(q_e) - \frac{k_1}{2.303} t \tag{4}$$

$$\frac{t}{q_t} = \frac{1}{q_e} t + \frac{1}{k_2 q_e^2} \tag{5}$$

where, q_e and q_t is the amount of 2,4-DCP adsorbed per unit mass of the AC at equilibrium and time t, respectively (mg g^{-1}); t is time (min); k_1 is the rate constant for pseudo-first-order (min^{-1}); k_2 is the rate constant for pseudo-second-order (g mg^{-1} min^{-1}).

The intraparticle diffusion model was used to identify the mechanism of the adsorption in this study.

$$q_t = k_{id} t^{0.5} + C \tag{6}$$

Table 1. ACs with their relative yield percentage, moisture, ash and pH

Sample	Yield (%)	Moisture content (%)	Ash content (%)	pH
AC1	32.39	4.67	8.37	5.80
AC2	34.41	4.95	10.30	5.95
AC3	37.10	5.36	11.69	5.88
AC4	38.85	6.09	13.36	6.18
AC5	33.51	7.03	14.84	6.12

where, k_{id} is the rate constant for intraparticle diffusion (mg g^{-1} $min^{0.5}$); C is the plot intercept.

RESULTS AND DISCUSSION

1. Physical Characterization

The yield percentage, moisture, ash content and pH of AC1-AC5 are shown in Table 1. The percentage of yield increased from 32.39% to 38.85% for AC1 to AC4, respectively, but then decreased to 33.51% for AC5. These results were consistent with the results of previous researchers [40,41]. The condensation (polymerization) reactions caused by the chemical agents, which promoted the formation of large polycyclic aromatics molecules in the activated products and hence the yield, increased when the ratio of the chemical agent increased [19]; but at higher impregnation ratio (1 : 5), excess $ZnCl_2$ widened the micropores into mesopores, which promoted the burning-off of the carbon matrix in the sample resulting in the decrease in the percentage of yield [41]. The moisture content of the prepared ACs varied from 4.67% until 7.03% (Table 1), which was relatively low and within the acceptable range [21]. Low moisture content of an adsorbent indicates the lower occupation of the active site or the pores of the adsorbent, and this affects the adsorption process significantly [43]. Hence, adsorption capacity of the AC increased with the decrease of moisture content. As shown in Table 1, the ash content increased as the impregnation ratio increased; this was similar to the trend observed by previous researchers [44]. Ash content of the AC was the residue that remained when the carbonaceous portion was burned off. The ash from plant waste consists mainly of minerals such as silica, aluminium, iron, magnesium and calcium. Ash in AC is not required and is considered to be an impurity [45]. However, in this study, the ash content in ACs was within the acceptable limit for commercial AC production, which was from 5% to 15% [46]. The important parameter for the adsorption process was the pH of the ACs. This was due to the distribution of the functional groups that were consistent with the pH of the AC [47]. The pH of the AC was measured at 50 °C due to the optimum adsorption temperature. The pH of the prepared activated carbons was determined to be slightly acidic; therefore, the activated carbon samples were classified as L-type carbon.

2. Surface Functional Group of AC

Fig. 1 and Fig. 2 show FTIR spectra of raw papaya seeds and all the samples of AC, respectively. From the FTIR analysis, the raw papaya seeds showed the presence of more oxygen-containing surface functional group compared to the prepared ACs. The adsorption bands at 3,434 cm^{-1} and 2,927 cm^{-1} were assigned to the stretching of O-H bonds for alcohol and stretching of C-H bonds for alkenes. The adsorption band at 2,856 cm^{-1} was associated with the C-H stretching vibration of methyl substituent in the lipid [48]. Sharp band at the 1,743 cm^{-1} indicated the C=O bonds of carboxylic acid or ester [49]. While the 1,645 cm^{-1} was the C=O stretching of carboxylic acid with intermolecular hydrogen bond [50]. The small peaks at 1,539 cm^{-1} indicated the presence of the C=C bonding in

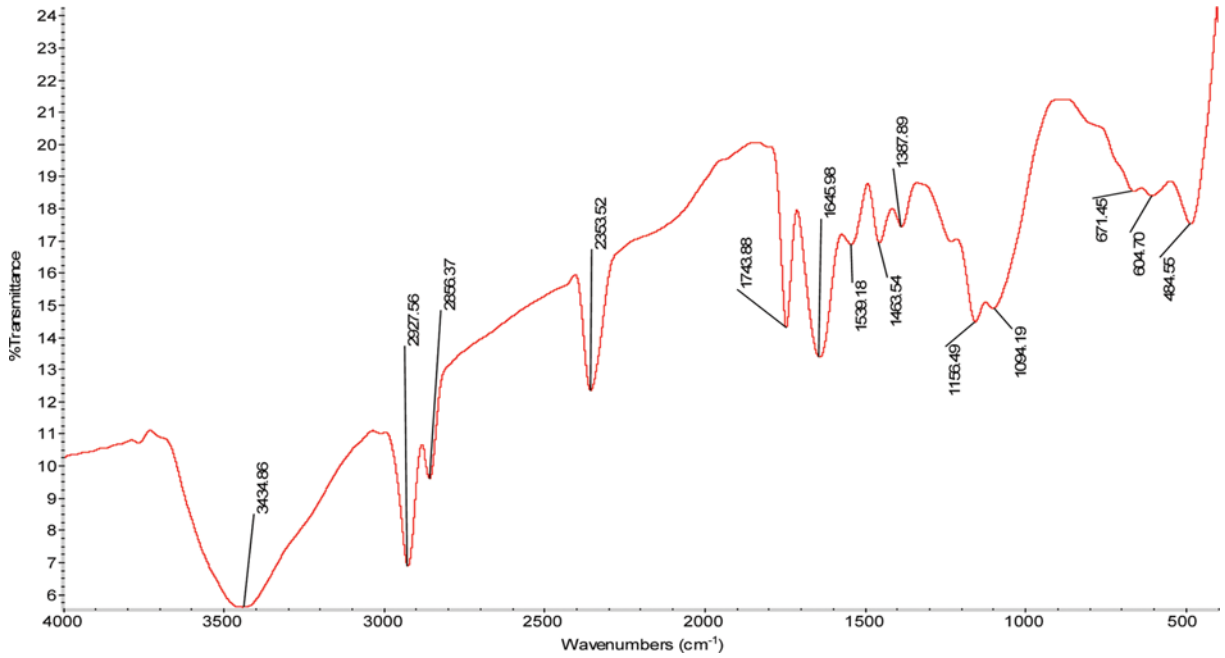

Fig. 1. FTIR spectra of raw papaya seeds.

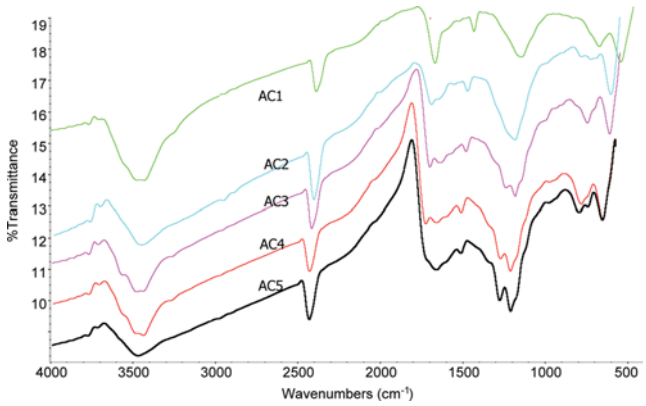

Fig. 2. FTIR spectra of the papaya seeds based activated carbons.

Table 2. Surface area, pore volume and pore size of AC2

Surface area	
Langmuir surface area, m^2/g	546
BJH method cumulative adsorption surface area, m^2/g	426
BJH method cumulative desorption surface area, m^2/g	495
Pore volume	
BJH method cumulative adsorption pore volume, cc/g	0.0018
BJH method cumulative desorption pore volume, cc/g	0.0020
Pore size	
Average pore diameter, Å	26.70
BJH method adsorption pore diameter (mode), Å	8.79
BJH method desorption pore diameter (mode), Å	9.14

the form of aromatics rings. The band at 1,156 and 1,094 cm^{-1} indicated the presence of the C-O stretching for the phenolic groups [51]. After the activation process, O and the H atoms were removed by the formation of H_2O and H_2 and released as gas. The adsorption bands of the AC showed smooth peak related to the C=O and O-H stretching.

3. Morphological Structure of AC

Fig. 3(a) shows the SEM micrographs of raw papaya seeds and Fig. 3(b)-(f) shows the ACs micrographs. For the raw papaya seeds, the adsorption of the adsorbate by the raw papaya seeds was possible due to the seeds containing heterogeneous, uneven, and rough surface, with heterogeneous cavities on the order of magnitude of mesopores and macropores [47]. However, many large pores in a honeycomb shape were developed on the surface of the activated carbon and a smooth melt surface appeared after the impregnation and activation process. The porous structures of the activated carbon were more favourable for the adsorption process. Hence, the activated carbons had higher adsorption capacity compared to the raw papaya seeds. The large pores were formed due to some of the volatiles compound being evolved [44].

4. Specific Surface Area and Pore-distribution

AC2 was selected for surface area and pore distribution analysis. The maximum Langmuir surface area of 546 m^2/g and the average pore diameter of 26.7 Å are comparable with the findings of other researchers [5-9,12]. Table 2 represents the porous and surface characteristics of AC2.

Fig. 4 shows the isotherms from N_2-sorption measurements of the papaya seeds, which contain specific information on the porosity of particles at the temperature of liquid nitrogen. Type I isotherm with H4 hysteresis loop was observed. This type of isotherm pattern is called single-molecule adsorption process, which is characterized by a continuous increase in the adsorption volume until the relative pressure reaches and exceeds a certain value. The presence of the H4 hysteresis loop is demonstrated by the horizontal and nearly parallel branch over a wide range of relative pressure (P/P_o) in Fig. 4. This confirms the existence of micropores in the

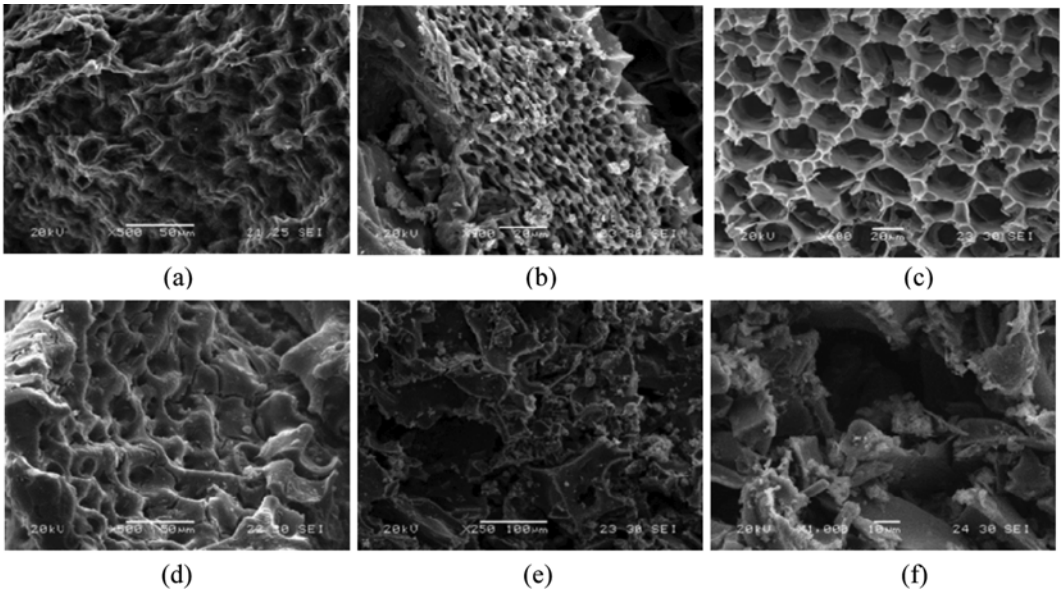

Fig. 3. The morphology of (a) raw papaya seeds (b) AC1 (c) AC 2 (d) AC3 (e) AC4 (f) AC5.

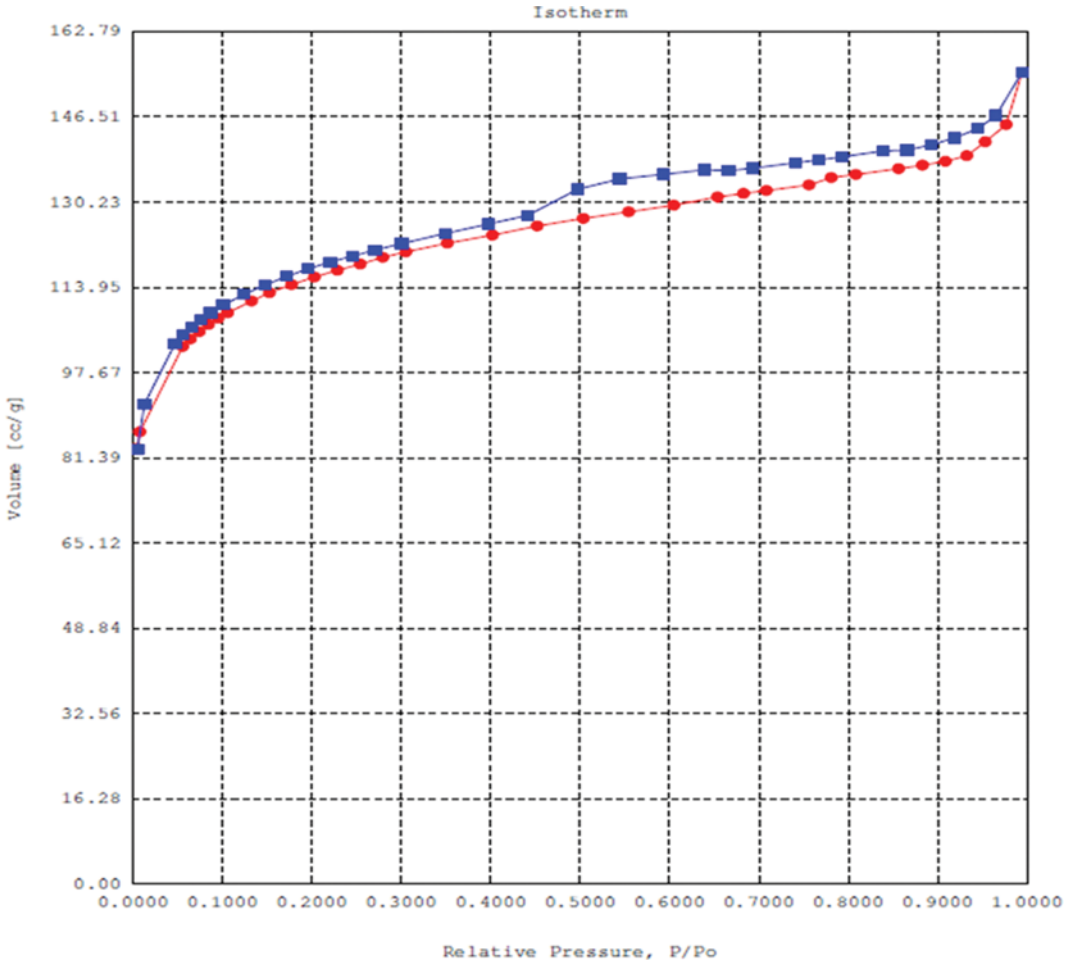

Fig. 4. Nitrogen adsorption-desorption isotherm for AC2.

slit-shaped pores structure, which is corroborated by the SEM data in Fig. 3(c). This isotherm is also corroborated by the Langmuir isotherm model, which indicates monolayer coverage with chemisorption adsorption properties due to the compliance with the pseudo-second-order reaction kinetics. This is a typical adsorption in microporous solids [7].

Table 3. Adsorption test results

Parameters		Adsorption percentage, %
Adsorption capacity	AC1	55.00
	AC2	91.75
	AC3	61.25
	AC4	36.75
	AC5	34.50
Adsorbent dosage, g	0.1	41.25
	0.3	64.00
	0.5	91.75
pH	3	84.25
	7	82.00
	9	80.50
Initial adsorbate concentration, mg L^{-1}	10	98.00
	20	95.50
	30	93.30
	40	91.75

5. Adsorption Study

The adsorption results are shown in Table 3. The optimum adsorption for the AC was at the impregnation ratio of 1 : 2, semi-carbonized at 300 °C for 1 h and activated for 500 °C for 2 h. This result was similar to previous researchers studying Tamarind wood for AC production [44]. As shown in Table 3, the adsorption percentage of 2,4-DCP increases is proportional to the increase in the amount of adsorbent dosage. This is because as the adsorbent dosage increased, there was an increase in availability of surface active site, which resulted from the increased dose and conglomeration of the carbons [52]. The contribution of the solution pH to the adsorption capacity was also studied. According to Table 3, the adsorption capacity of 2,4-DCP decreased with the increase in the pH of the solution, with the highest uptake achieved at pH 3. At this pH, the concentration of 2,4-DCP decreased from initial concentration of 40 to 6.3 mg/L. While, the lowest uptake was recorded at pH 9, where the concentration of 2,4-DCP dropped until 7.8 mg/L. This observation was similar to the research done previously [2] in which the adsorption of 2,4-DCP was favorable under

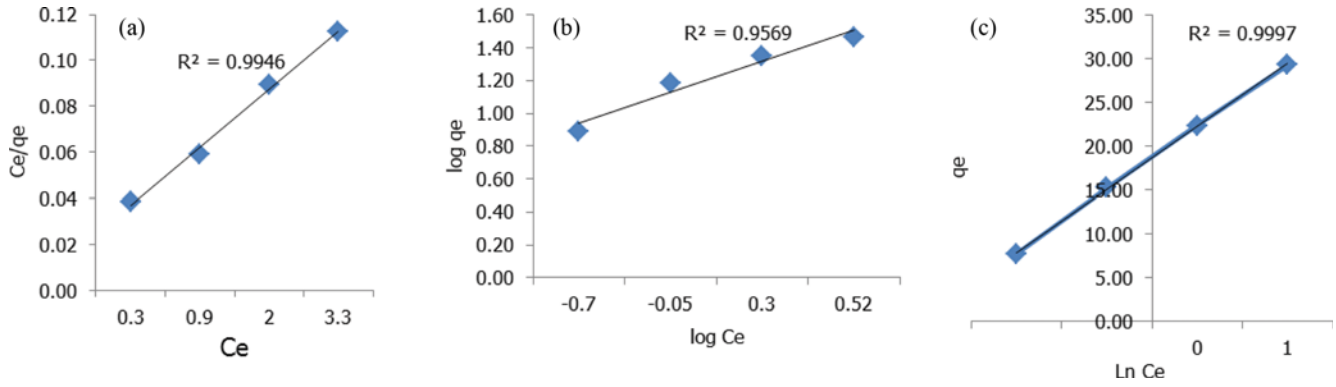

Fig. 5. (a) Langmuir isotherm (b) Freundlich isotherm (c) Temkin isotherm.

acidic condition. The behavior clearly suggests that the adsorption was dependent on the interaction between undissociated organic compounds and the organophilic nature of the adsorbent surface. As shown in Table 2, an increase in the initial concentration led to an increase in the amount of 2,4-DCP adsorbed on AC. This may be attributed to an increase in the driving force of the concentration gradient with the increase in the initial 2,4-DCP concentration [2].

6. Adsorption Isotherm Study

Adsorption isotherm was identified under the equilibrium conditions. When the adsorption process reached equilibrium, a distribution between the solid phase (adsorbent) and the liquid phase (adsorbate) was indicated according to different isotherm models. A suitable model was identified by the isotherm data analysis and fitted the data into different models [2]. In this study, the Langmuir and Freundlich models were used to describe the relationship between the equilibrium concentration and the amount of adsorbate adsorbed. The application of the models was justified by comparing the correlation coefficient value (R^2) of the graph. The plot for Langmuir, Freunlich and Temkin isotherm of the AC2 is shown in Fig. 5(a), (b), (c).

As shown in Fig. 5, the data fitted both Langmuir and Freundlich isotherms well, both R^2 were >0.9, but the Langmuir isotherm was more preferable. The correlation coefficient, R^2 from the Langmuir isotherm (0.9946) was larger than the R^2 from the Freundlich isotherm (0.9569). Therefore, the adsorption of the AC fulfilled the Langmuir isotherm. The Temkin isotherm contained a factor that explicitly takes into account adsorbent-adsorbate interactions. The correlation coefficient, R^2, from the Temkin isotherm (0.9997) indicated the adsorption process fulfilled the isotherm better than the Langmuir isotherm.

7. Adsorption Kinetics Study

A comparison for the adsorption kinetics between the pseudo first-order and pseudo second-order is illustrated in Fig. 6(a), (b).

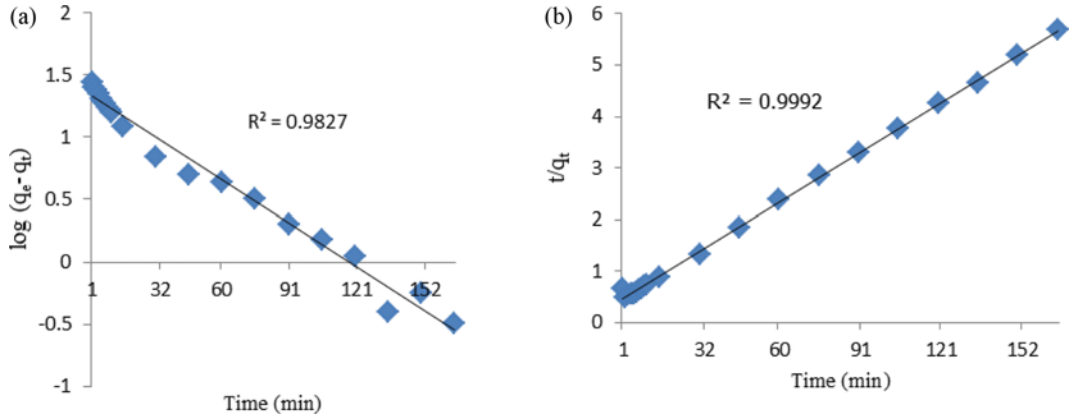

Fig. 6. (a) Pseudo first-order plot (b) pseudo second-order plot.

Table 4. Adsorption kinetics data

k_1 (min^{-1})	$q_{e,exp}$ mg g^{-1}	$q_{e,cal}$ mg g^{-1}	R^2	k_2 g mg^{-1} min^{-1}	$q_{e,exp}$ mg g^{-1}	$q_{e,cal}$ mg g^{-1}	R^2
Pseudo-first order				Pseudo-second order			
0.026	29.36	21.988	0.9827	2.29×10^{-4}	29.36	31.545	0.9992

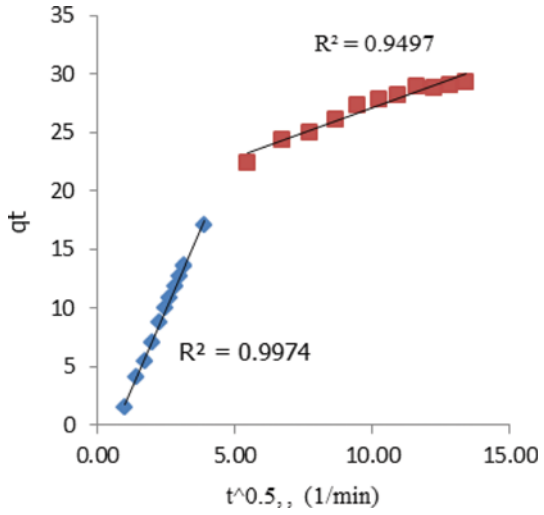

Fig. 7. The intraparticle diffusion model of the AC2.

A linear graph was plotted for both of the kinetics models by using the linear form of the pseudo first-order and pseudo second-order.

From Fig. 6, the correlation coefficient value for the pseudo second-order was 0.9992, while for the pseudo-first order was 0.9827. The data fitted the pseudo second-order well, indicating that the adsorption mechanism depends on both the adsorbate and the adsorbent. The adsorption process followed chemisorption, which involves the valence forces through the sharing or exchange of electrons [38-53]. Table 4 represents the adsorption kinetics data.

Intraparticle diffusion model was tested to identify the diffusion mechanism. The boundary layer effect was identified by collaboration of the y-intercept. The higher the y-intercept, the contribution of the surface sorption is higher in the rate-controlling step. Fig. 7 illustrates the plots of q_t versus $t^{0.5}$ for of 2, 4-DCP initial concentrations of 40 mg/L. It was observed that the linear plots at each concentration did not pass through the origin. This indicated that intraparticle diffusion was not the only rate controlling step. Such trend was reported by several researchers in their previous investigation on adsorption [2].

According to Fig. 7, the adsorption process was separated into two stages. The sharper slope is due to the external surface adsorption or instantaneous adsorption, while the second stage is the gradual adsorption stage where the intra-particle diffusion occurs simultaneously in the adsorption mechanism.

CONCLUSION

Papaya seeds, which are agriculture waste with no economic value, proved to be very suitable as precursors for the preparation of high adsorption capacity AC. High percentage yields were achieved, which ranged from 32.39% to 38.85%, the moisture content of the AC was below 7.03% while the ash content was below 14.84%, and the pH of the AC was between 5 and 7, indicating that this material is a suitable precursor for AC production. The surface functional groups of the papaya seeds and the ACs were compared; some of the C=O, O-H functional groups were absent in ACs due to the activation process that evolved the volatile matters. The morphology studies indicated that the presence of honeycomb-like structure indicated rich pores were present in the AC compared to the raw papaya seeds. The maximum BET surface area of the optimized AC (AC2) was 546 m^2/g and its adsorption efficiency of the 2,4-DCP was 91.75%. The adsorption process of the 2,4-DCP by AC2 fitted well in Langmuir isotherm model, which yielded an R^2 of 0.9946, while adsorption kinetic data fitted the pseudo-second-order with R^2 of 0.9992. This indicated that the adsorption process was a chemisorption occurring on the monolayer of the adsorbent. The intraparticle diffusion model proved the mechanism of adsorption was separated into two stages: the instantaneous stage and the gradual adsorption stage. This study opens a new possibility of employing papaya seeds for the production of activated carbon and would generate a waste to wealth opportunity for enterprising individuals.

ACKNOWLEDGEMENT

This research was supported by the Research Management Center of Universiti Malaya in collaboration with the Center of Research and Innovation of Universiti Malaysia Sabah (Grant No. GL0111 or UM Project code: CG071-2013). These contributions are gratefully acknowledged.

REFERENCES

1. I. A. Tan, A. L. Ahmad and B. H. Hameed, *J. Hazard. Mater.*, **153**, 709 (2008).
2. F. W. Shaarani and B. H. Hameed, *Desalination*, **255**, 159 (2010).
3. A. O. Olaniran and E. O. Igbinosa, *Chemosphere*, **83**, 1297 (2011).
4. P. Nowicki, J. Kazmierczak and P. Robert, *Powder Technol.*, **269**, 312 (2015).
5. C. G. Joseph, A. Bono, S. M. Anisuzzaman and D. Krishnaiah, *J. Appl. Sci.*, **14**, 3182 (2014).
6. D. Krishnaiah, S. M. Anisuzzaman, A. Bono and R. Sarbatly, *J. King Saud University - Sci.*, **25**, 251 (2013).
7. S. M. Anisuzzaman, C. G. Joseph, Y. H. Taufiq-Yap, D. Krishnaiah and V. V. Tay, *J. King Saud University - Sci.*, **27**, 318 (2015).
8. S. M. Anisuzzaman, C. G. Joseph, W. M. A. W. Daud, D. Krishnaiah and H. S. Yee, *Int. J. Ind. Chem.*, **6**, 9 (2015).
9. S. M. Anisuzzaman, C. G. Joseph, D. Krishnaiah, A. Bono and L. C. Ooi, *Water Sci. Technol.*, **72**, 896 (2015).
10. V. K. Gupta and A. Nayak, *Chem. Eng. J.*, **180**, 81 (2012).
11. A. Mittal, D. Kaur, A. Malviya, J. Mittal and V. K. Gupta, *J. Colloid Interface Sci.*, **337**, 345 (2009).
12. I. A. W. Tan, A. L. Ahmad and B. H. Hameed, *J. Hazard. Mater.*, **164**, 473 (2009).
13. J. Fan, J. Zhang, C. Zhang, L. Ren and Q. Shi, *Desalination*, **267**, 139 (2011).
14. R. H. Hesas, Roozbeh, W. M. A. W. Daud, J. N. Sahu and A. Arami-Niya, *J. Anal. Appl. Pyrol.*, **100**, 1-1.1 (2013).
15. M. J. Ahmed and S. K. Theydan, *J. Anal. Appl. Pyrolysis*, **100**, 253 (2013).
16. I. Okman, S. Karagöz, T. Tay and M. Erdem, *Appl. Surf. Sci.*, **293**, 138 (2014).
17. K. Y. Foo and B. H. Hameed, *Chem. Eng. J.*, **170**, 338 (2011).

18. A. Özhan, S. Ömer, M. M. Küçük and C. Saka, *Cellulose*, **21**, 2457 (2014).
19. F. Boudrahem, F. Aissani-Benissad and H. Aït-Amar, *J. Environ. Manage.*, **90**, 3031 (2009).
20. S. Uçar, M. Erdem, T. Tay and S. Karagöz, *Appl. Surf. Sci.*, **255**, 8890 (2009).
21. R. G. Pereira, C. M. Veloso, N. M. da Silva, L. F. de Sousa, R. C. F. Bonomo, A. O. de Souza, M. O. da Guardo Souza and F. R. da Costa Ilhéu, *Fuel Process. Technol.*, **126**, 476 (2014).
22. M. Olivares-Marín, C. Fernández-González, A. Macías-García and V. Gómez-Serrano, *Appl. Surf. Sci.*, **252**, 5967 (2006).
23. S. M. Alshehri, M. Naushad, T. Ahamad, Z. A. AL Othman and A. Aldalbahi, *Chem. Eng. J.*, **254**, 181 (2014).
24. A. Kumar, C. Guo, G. Sharma, D. Pathania, M. Naushad, S. Kalia and P. Dhiman, *RSC Adv.*, **6**, 13251 (2016).
25. A. A. Alqadami, M. Naushad, M. A. Abdalla, T. Ahamad, Z. A. AL Othman and S. M. Alshehri, *RSC Adv.*, **6**, 22679 (2016).
26. Z. A. Al Othman and M. Naushad, *Environ. Sci. Pollut. Res.*, **20,** 3351 (2013).
27. M. Naushad and Z. A. Al Othman, *Desalination Water Treatment*, **53**, 2158 (2015).
28. A. Kumar, G. Sharma, M. Naushad, P. Singh and S. Kalia, *Ind. Eng. Chem. Res.*, **53**, 15549 (2014).
29. M. Naushad, Z. A. AL Othman, M. R. Awual, M. M. Alam and G. E. Eldesoky, *Ionics*, **21**, 2237 (2015).
30. M. Naushad, Z. A. AL Othman, G. Sharma, Inamuddin, *Ionics*, **2**, 1453 (2015).
31. R. Bushra, M. Naushad, R. Adnan and M. Rafatullah, *J. Ind. Eng. Chem.*, **21**, 1112 (2015).
32. M. Naushad, Z. A. AL Othman, Inamuddin and H. Javadian, *J. Ind. Eng. Chem.*, **25**, 35 (2015).
33. M. Naushad, T. Ahamad, G. Sharma and A. A. Ahmed, *Chem. Eng. J.*, **300**, 306 (2016)**.**
34. A. Gundogdu, C. Duran, H. B. Senturk, M. Soylak, M. Imamoglu and Y. Onal, *J. Anal. Appl. Pyrolysis*, **104**, 249 (2013).
35. A. Gundogdu, C. Duran, H. B. Senturk, M. Soylak, D. Ozdes, H. Serencam and M. Imamoglu, *J. Chem. Eng. Data*, **57**, 2733 (2012).
36. C. Duran, D. Ozdes, A. Gundogdu, M. Imamoglu and H. B. Senturk, *Anal. Chim. Acta*, **688**, 75 (2011).
37. C. Srinivasakannan and M. A. B. Zailani, *Biomass Bioenergy*, **27**, 89 (2004).
38. L. J. Kennedy, J. J. Vijaya, K. Kayalvizhi and G. Sekaran, *Chem. Eng. J.*, **132**, 279 (2007).
39. J. Gañán-Gómez, A. Macías-García, M. A. Díaz-Díez, C. González-García and E. Sabio-Rey, *Appl. Surf. Sci.*, **252**, 5976 (2006).
40. J. P. Wang, Y. Z. Chen, H. M. Feng, S. J. Zhang and H. Q. Yu, *J. Colloid Interface Sci.*, **313**, 80 (2007).
41. Q. Qian, M. Machida and H. Tatsumoto, *Bioresour. Technol.*, **98**, 353 (2007).
42. S. Farzad, V. Taghikhani, C. Ghotbi, B. Aminshahidi and E. N. Lay, *J. Natural Gas Chem.*, **16**, 22 (2007).
43. L. Zhou, L. Ming, Y. Sun and Y. Zhou, *Carbon*, **39**, 773 (2001).
44. I. Ozdemir, M. Şahin, R. Orhan and M. Erdem, *Fuel Process. Technol.*, **125**, 200 (2014).
45. J. Acharya, J. N. Sahu, C. R. Mohanty and B. C. Meikap, *Chem. Eng. J.*, **149**, 249 (2009).
46. K. J. Silgado, G. D. Marrugo and J. Puello, *Chem. Eng. Transactions*, **37**, 721 (2014).
47. S. Yenisoy-Karakaş, A. Aygün, M. Güneş and E. Tahtasakal, *Carbon*, **42**, 477 (2004).
48. C. T. Weber, E. L. Foletto amd L. Meili, *Water, Air Soil Pollution*, **224**, 1427 (2013).
49. E. I. Unuabonah, G. U. Adie, L. O. Onah and O. G. Adeyemi, *Chem. Eng. J.*, **155**, 567 (2009).
50. F. A. Pavan, E. S. Camacho, E. C. Lima, G. L. Dotto, V. T. A. Branco and S. L. P. Dias, *J. Environ. Chem. Eng.*, **2**, 230 (2014).
51. N. F. Cardoso, E. C. Lima, I. S. Pinto, C. V. Amavisca, R. Betina, R. B. Pinto, W. S. Alencar and S. F. P. Pereira, *J. Environ. Manage.*, **92**, 1237 (2011).
52. M. M. Karim, A. K. Das and S. H. Lee, *Analytica Chimica Acta*, **576**, 37 (2006).
53. L. Wang, J. Zhang, R. Zhao, C. Zhang, L. Cong and L. Ye, *Desalination*, **266**, 175 (2011).